Oil & Gas Science and Technology – Rev. IFP, Vol. 58 (2003), No. 1, pp. 63-78
Copyright © 2003, Éditions Technip

Fuel/Air Mixing Process and Combustion in an Optical Direct-Injection Engine

J.F. Le Coz[1], J. Cherel[1] and S. Le Mirronet[2]

1 Institut français du pétrole, division Techniques d'applications énergétiques, 1 et 4, avenue de Bois-Préau, 92852 Rueil-Malmaison Cedex - France

2 ALTRAN Technologies, 58, boulevard Gouvion-Saint-Cyr, 75858 Paris Cedex 17 - France

e-mail: j-francois.le-coz@ifp.fr - jerome.cherel@ifp.fr

Résumé — Préparation du mélange et combustion dans un moteur à injection directe avec accès optique — Sur un moteur à injection directe d'essence muni d'accès optique, et fonctionnant en mélange stratifié, nous étudions le mélange air/carburant dans la chambre de combustion par fluorescence induite par nappe laser et nous corrélons ses caractéristiques avec le déroulement de la combustion. Trois conditions caractéristiques faisant varier le moment de l'injection sont examinées. La concentration moyenne de carburant à la bougie au moment de l'allumage est élevée lorsque l'injection est proche de l'allumage. On distingue même un mouillage de la bougie conduisant à des ratés d'étincelle. Lorsque l'on avance l'injection, on s'approche de conditions stœchiométriques, qui offrent la meilleure qualité de combustion. Une avance excessive produit en revanche des conditions à la fois pauvres et instables, provoquant une combustion plus lente et plus fluctuante. Dans ce cas, les corrélations cycle à cycle entre concentration en carburant à la bougie et initiation de la combustion sont fortes. Le meilleur réglage du moteur est observé lorsque l'on atteint une richesse moyenne de 1 à la bougie au moment de l'allumage et que l'on y maximise la probabilité d'avoir une richesse voisine de 1 à tous les cycles.

Abstract — Fuel/Air Mixing Process and Combustion in an Optical Direct-Injection Engine — *Fuel/air mixing is analysed on an optical gasoline direct-injection engine. The fuel concentration field is measured using a laser-induced fluorescence technique. Three conditions, which vary injection timing while keeping constant the ignition timing, are investigated. A qualitative correlation is made between the local fuel/air ratio near the spark plug with ignition and combustion in the chamber. It is found that the mean concentration at the ignition point is high when the delay between injection and ignition is short. In some cycles, liquid fuel covers the electrodes resulting in frequent misfires. The best operating point is achieved with near-stoichiometric conditions at the ignition point, and a moderate concentration cyclic variability. On the contrary, early injection timing gives lean conditions and large cyclic variations at the ignition point. Moreover, the mixture is more dilute in the chamber, and combustion is slow and unstable. Cycle to cycle correlation between fuel concentration near the spark gap and combustion initiation shows that locally lean conditions give very slow combustion.*

LIST OF ACRONYMS

GDI	gasoline direct injection
UV	ultraviolet
BMEP	best mean effective pressure
TDC	top dead center
CAD	crank angle degrees
BTDC	before top dead center
F/A (equ.) or Φ	fuel/air (equivalence) ratio.

INTRODUCTION

The development of direct-injection gasoline engines running in the stratified-charge mode requires a precise control of the injection process, fuel evaporation and stratification [1]. A short time is available for mixing air and fuel, and fuel is likely to impinge the walls, because jet penetration is long compared to the chamber dimensions. Short deviations of the fuel spray or small changes in the injection timing lead frequently to large changes in the flammability and in engine emissions, like unburned hydrocarbons. Combustion is also particular because the flame does not propagate throughout the whole chamber as in conventional homogeneous engines. Very different technological concepts are coming out. The way to control the rich cloud position and extension in the chamber are numerous [2]. Wall guiding can be used to keep a rich zone in a piston bowl, transport of the spray by the airflow can also be used. Swirl is for example used in the *Toyota* engine [3], tumble in the *Mitsubishi* one [4, 5], or a combination in the *Nissan* [6]. In other concepts, the ignition point is located on the spray side; they are called sometimes narrow spacing or spray-guide because the spark plug is close to the injector in the cylinder head. This shows that the optimal configuration has not been found yet. Internal phenomena are complicated, which explains why combustion history and emissions are not understood enough.

Consequently, a thorough understanding of the internal phenomena is needed to learn about the parameters that control the combustion. This work uses an engine equipped with large optical access, that allows acquiring images of the fuel concentration in the combustion chamber. The study aims to gain knowledge on the phenomena taking place, using advanced diagnostic tools, rather than obtaining operating conditions rigorously equivalent to a production engine. We will determine the progress of fuel evaporation at spark timing, the fuel concentration fields generated, and how ignition and combustion develops in the stratified zone. The information brought by this work will support the development of new engine concepts using direct-injection, and furthermore, validate 3D modeling that have become efficient prediction tools [7, 8].

1 EXPERIMENTAL SET-UP

A single-cylinder engine with large optical access is used. It is based on a homogeneous charge optical 4-valve engine, which was modified to perform gasoline direct injection[1] (GDI). A small window is located in the cylinder head, and a large window in the elongated piston; the Bowditch's concept used by this engine gives optical access to the combustion chamber from the bottom of the engine, with a 45 degree mirror fixed below the transparent piston. The chamber geometry is simpler than that of a common GDI engine, because the injector is central and the piston surface is flat (*Fig. 1*). The injector is located in the normal spark plug position. The spark plug is horizontal, located on the side opposite to the cylinder head window, with long electrodes. The electrode gap is 0.7 mm wide and located 13 mm below the injector nozzle (*Fig. 2*).

The intake valves cannot rotate on their seats and are equipped with shrouds that force tumble in the chamber. The tumble number of the engine flow field is about 2.5.

1 Gasoline direct injection referred to as GDI later on. A list of all acronyms is given in this paper.

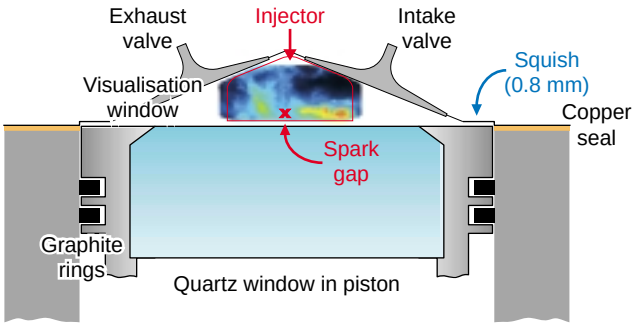

Figure 1

Optical access through the combustion chamber.

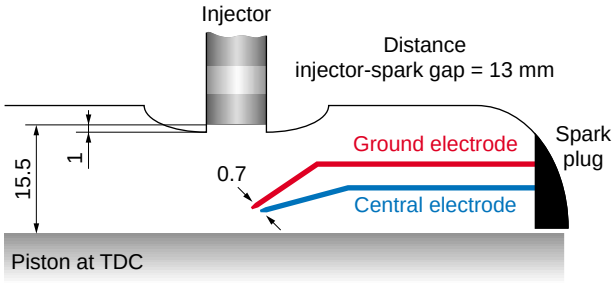

Figure 2

Chamber geometry.

Laser-induced fluorescence is used to track the fuel spray and the rich pocket motion. Excitation is done by an UV pulsed YAG laser with a wavelength of 266 nm and a pulse energy of 80 mJ. A system made of cylindrical and spherical lenses transforms the original 7 mm diameter laser beam in a laser sheet that is 30 mm wide and less than 0.5 mm thick. The laser sheet is directed to the 45 degree mirror in the engine bottom, and crosses the combustion chamber vertically (*Fig. 3*). It follows the symmetry plane and intersects the injector nozzle when reaching the cylinder head roof. A tracer is introduced in the fuel. This tracer when illuminated by the laser sheet yields fluorescence that is collected through the window in the cylinder head and imaged on an intensified CCD camera. An optical filter matched to the fluorescence band of the tracer rejects the excitation laser wavelength. Thus, background noise coming from laser light reflections on the walls is minimised. An image of the fuel concentration in the laser sheet plane is obtained on the camera.

The compression ratio was slightly increase from 9 to 10.5 to represent more closely the conditions of a GDI engine. Putting thicker seats increased the valve recess. The squish zone height was reduced to the minimum acceptable value (0.8 mm).

The engine characteristics are summarised in Table 1.

TABLE 1

Engine characteristics

Displacement volume	441 cm^3
Bore	82 mm
Stroke	83.5 mm
Connecting rod	141.45 mm
Compression ratio	10.5

2 LASER-INDUCED FLUORESCENCE SET-UP

Previous work done at *IFP* used exciplex tracers, a mixture of benzene and triethylamine (TEA). The boiling points of these species are close to that of iso-octane, and the evaporation process is correctly probed. It has been demonstrated [9, 10] that the combination of these tracers forms an exciplex molecule in the liquid phase under illumination by strong laser light at 248 or 266 nm. With 2.9% benzene and 4.1% TEA a very large spectral separation of TEA/benzene (tracing the vapour) and exciplex (tracing the liquid) occurs, enabling isolation of vapour from liquid fluorescence by the use of an optical filter centred on 290 nm [10, 11].

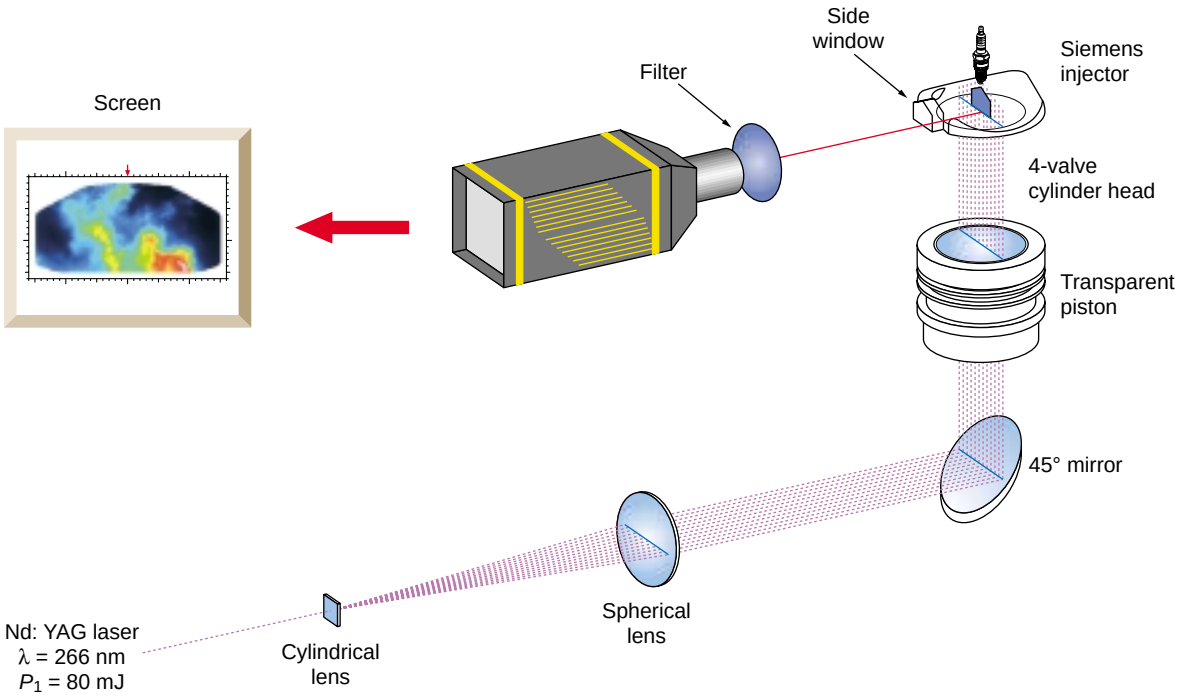

Figure 3

Laser-induced fluorescence arrangement.

We continued with this combination, and compared their fluorescence yield with that of more common tracers from the ketone family. The comparison was done in the engine, injecting during the intake stroke in order to achieve a homogeneous concentration field in the chamber. The engine was supplied either with air or with nitrogen, because oxygen is known to cause quenching of fluorescence.

The fuel is visualised near top dead center (TDC), at a crank-angle where almost all the fuel is vapour. The fuel used in all the tests is pure iso-octane, specie that is absolutely not fluorescent with our excitation wavelength of 266 nm. The tracers used are listed in Table 2. The exciplex mixture is made of 2.9% benzene and 4.1% TEA. A band-pass filter centred on 300 nm was used to collect only the vapour phase fluorescence. These figures are the result of an optimisation done in the past, which showed that the overlap of the fluorescence bands of the liquid and vapour phases is minimised with these concentrations [12]. The others tracers are all ketones, with different boiling points. Their concentration in iso-octane was 5%, and a long-pass filter with a cut-off of 400 nm was used, because the fluorescence band is between 400 and 470 nm with a maximum near 430 nm [13].

All of the tracers were excited using the same laser and optical arrangement, except the filter.

TABLE 2

Physical properties of tracers compared with iso-octane

Species	Mol. weight	Boiling point
iso-octane	***114.23***	***99°C***
benzene	*76.115*	*81°C*
TEA	*101.19*	*89°C*
3-pentanone	*86.13*	*102°C*
3-hexanone	100.16	125°C
2-hexanone	100.16	128°C

The exciplex tracer combination is very powerful in nitrogen, giving 3 times more fluorescence than 3-pentanone for example (*Fig. 4*). But it is strongly quenched by oxygen. Therefore, it will be used in the engine tests without combustion, to characterise precisely the fuel concentration field before spark timing.

Ketones showed negligible quenching by oxygen, the signal to noise ratios keeping almost identical with air or nitrogen. Among them, we will use 3-pentanone that represents a compromise between fluorescence yield and boiling point matching with iso-octane. 3-pentanone is suited for engine tests with combustion for correlating the fuel field near spark timing with combustion. At these late crank-angles fuel is very probably totally evaporated, so that the fact that liquid cannot be discriminated from vapour is not important.

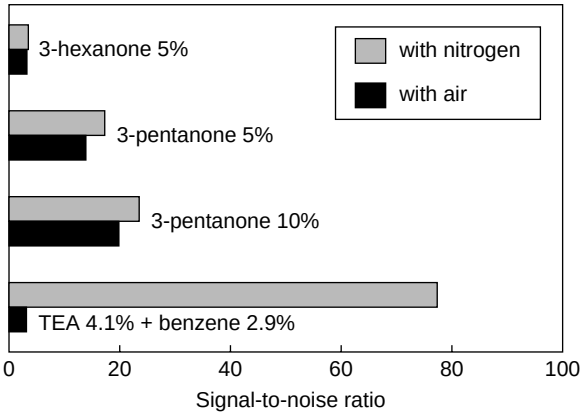

Figure 4

Signal-to-noise ratios obtained in the engine fed with air or nitrogen.

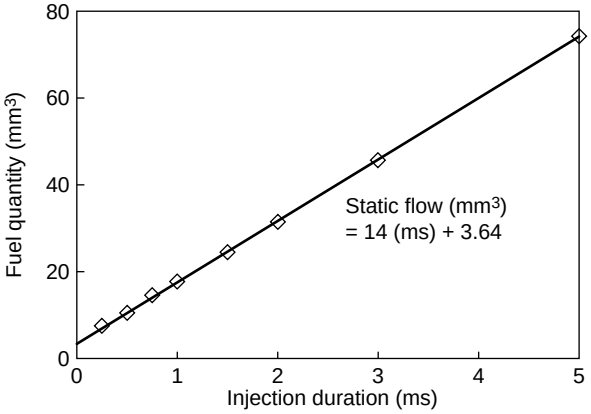

Figure 5

Flow rate of the injector.

3 INJECTOR SPRAY CHARACTERISATION

Considering that the short distance between the piston surface and the injector nozzle, a wide spray is recommended to lessen spray-wall impact. For this reason, we selected an injector from *Siemens* with a spray cone angle of 70°. The flow rate given by the supplier is 9.96 g/s with 7 MPa fuel pressure using *n*-heptane.

The flow rate of the injector was measured with iso-octane, using an EMI2 metering apparatus from *EFS*. The downstream pressure was fixed to 0.5 MPa, the upstream, to 7.5 MPa. The flow rate is 9.7 g/s with iso-octane (*Fig. 5*).

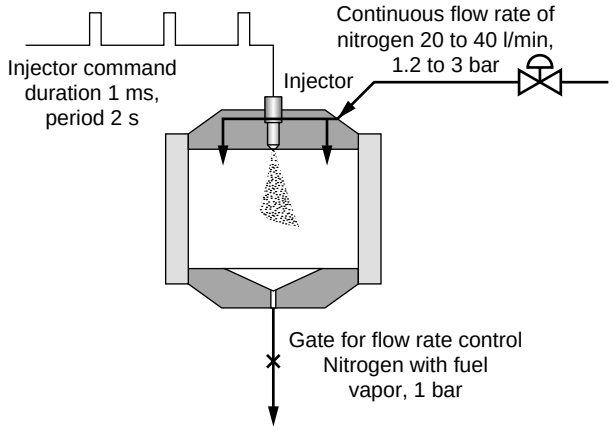

Figure 6

Injection cell, operating mode.

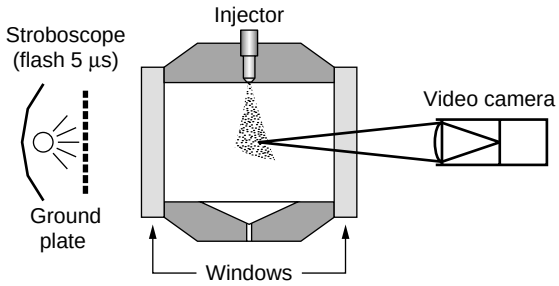

Figure 7

Spray imaging set-up.

Injection was done in a pressurised cell equipped with quartz windows. A continuous flow rate of nitrogen was sent through the cell and was set by a gate on the outlet port. The nitrogen flow scavenges vaporised fuel between each injection (*Fig. 6*). Fuel injection was done with a duration of 1 ms and a period of 2 s. This allowed a large part of the fuel to drain off between two injection shots, as could be checked experimentally.

Light extinction is used to visualise the spray shape. A stroboscope illuminates a ground plate behind the spray and a video camera records the images (*Fig. 7*). Images shown in this paper are mean images of 20 injection pulses, normalised by a mean reference image taken without the spray.

Two conditions with different pressure levels in the cell are tested, at 0.1 and 0.3 MPa to represent the gas density in a combustion chamber with the homogeneous and stratified mixture modes, respectively. Images of spray development obtained by light extinction are given in Figures 8 and 9. At 0.1 MPa, the spray is a hollow cone close to the injector. This cone tends to be filled farther downstream. The spray is optically dense, because the droplets formed are small, with a Sauter's mean diameter of about 20 µm. The spray motion forms a large toroidal structure, which is visible through the side recirculations at times after 1.5 ms on the images. At 0.3 MPa, it becomes narrower and denser. Stronger air entrainment from the sides is responsible for spray collapsing. This is a general behaviour of sprays produced by pressure swirl injectors [14]. The droplet mean diameter was shown to slightly increase with cell pressure in previous work [15]. The overall droplet surface is smaller, and the higher optical density is caused by a higher droplet

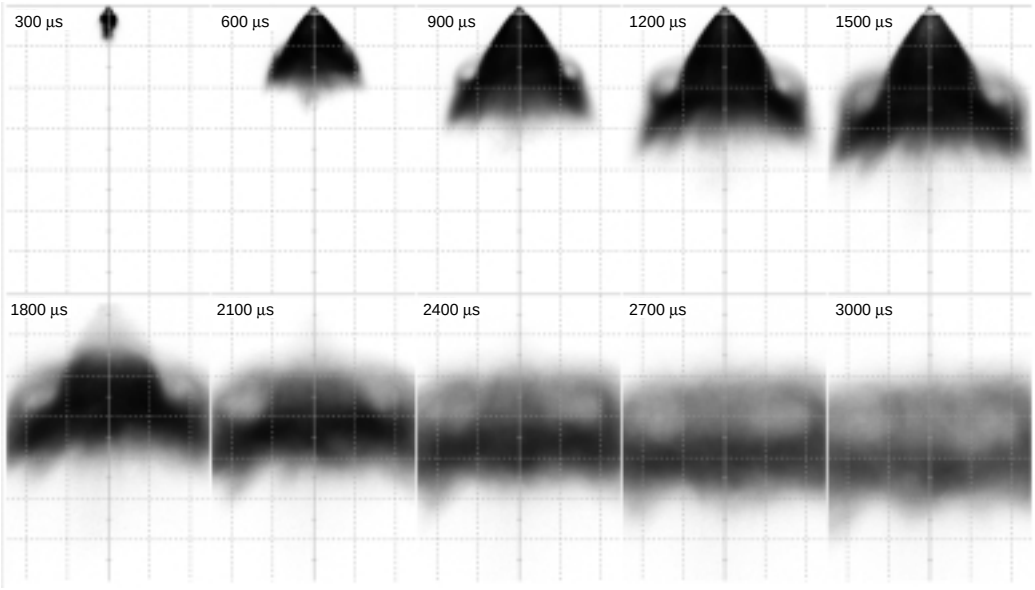

Figure 8

Spray development in the low pressure condition (0.1 MPa).

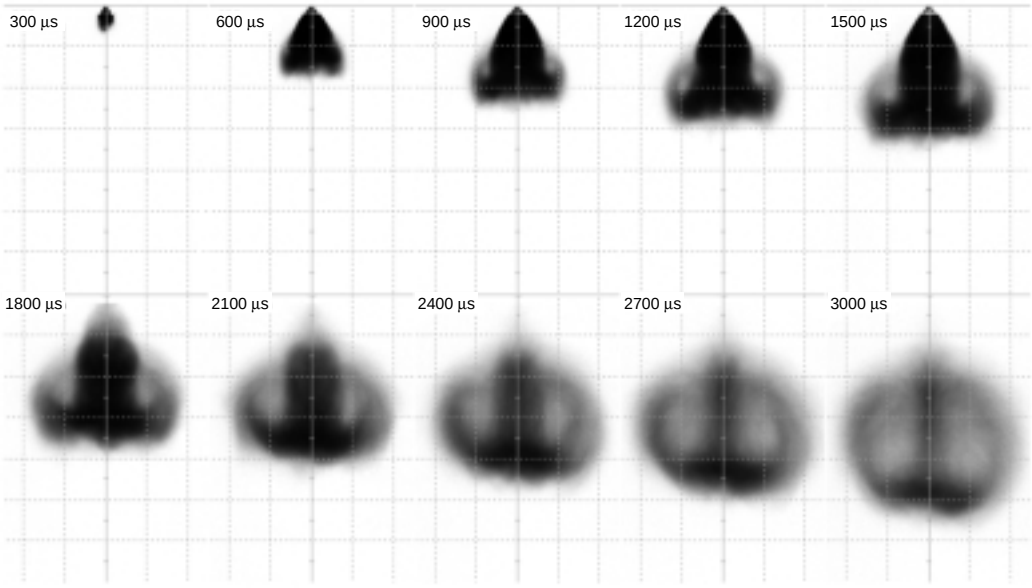

Figure 9

Spray development in the high pressure condition (0.3 MPa).

concentration. The angle and penetration of the sprays were calculated upon these images (*see Table 3*). In the low pressure condition, the spray cone angle measured on the extinction images is 7 degrees less than the value given by the manufacturer (63 instead of 70). With a 0.3 MPa cell pressure, the spray angle is much smaller. Jet penetrations are not very different however, because a balance occurs between better overall momentum conservation due to a smaller spray angle and higher drop braking due to higher ambient density. The result is a slightly smaller penetration with 0.3 MPa.

The spray penetration curve shown in Figure 10 indicates than the spray would impact the piston top surface in a short delay after the onset of injection, *i.e.* 4 CAD.

4 COMBUSTION MAPPING

We examined the combustion behaviour of the engine operating in the stratified charge mode. The engine running conditions are 1200 rpm, volumetric efficiency 0.9 and overall mean fuel/air equivalence ratio 0.3. The fuel injection pressure was 0.7 MPa, and the injection duration, adjusted to reach a fuel/air ratio of 0.3 was 713 µs.

The spark and injection timings were varied independently in a test matrix, and in each condition, the mean and standard deviation of BMEP were acquired. The percentage of misfiring cycles was also measured. The results can be summarised as followed. First, a zone with unstable combustion but no misfires is observed, with early injection and late spark timing. On the opposite side, a higher BMEP but a large percentage of misfiring cycles is observed with late injection and early spark timing. An optimum combustion is generally obtained when the delay between injection and ignition is about 13 CAD. Thus, we selected for the rest of this study three particular conditions that makes vary this delay, with a constant spark timing. Those results are detailed in Table 4.

TABLE 3

Spray characteristics at 1.5 ms after injection command

	0.1 MPa cell pressure				0.3 MPa cell pressure			
	Mean	rms	Min.	Max.	Mean	rms	Min.	Max.
Angle at 15 mm (degree)	62.5	0.73	61.3	63.9	48.9	0.63	48.3	50.4
Cone penetration (mm)	37.30	0.37	36.74	37.91	32.91	0.69	32.09	33.95
Prejet penetration (mm)	44.35	1.07	42.56	46.05	35.12	0.56	34.19	35.81

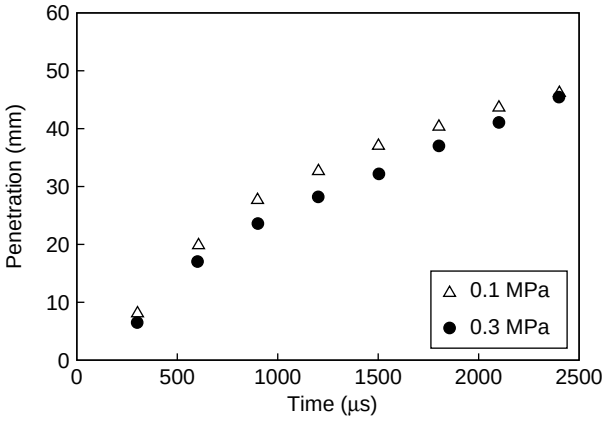

Figure 10

Spray penetration curves.

The optimal condition, who gave the best BMEP together with the minimum standard deviation and no misfire, was named A. Two other conditions, typical of nonoptimal combustion behaviour were selected, named B for a late or retarded injection, and C for an early or advanced injection.

5 SPARK VISUALISATIONS

The spark discharge was visualised through the transparent piston. Initially, the objective was to verify that the arc develops in the gap between the electrode tips. The three selected conditions and a fourth one without injection were investigated. The latter allows to isolate the flow field effect.

We show in Figure 11 typical single images in a square field, 10 mm wide, and the probability of finding a spark in the same field. Without injection, the spark is convected towards the right side. This reflects the strong tumble motion in this engine, that generates a flow from the exhaust to the intake side near the piston surface, where the electrode gap is located. With injection however, no mean convection is visible, probably because a flow is induced by the spray. In the optimal and the early injection conditions A and C, the spark looks sharp, and can deviate from the gap by 3 mm. In the late injection condition B, the spark looks blurred and less intense. We could see also that no spark occurs in some cycles. These features indicate that the spark location is just in the liquid spray, and that a liquid film very probably covers the electrodes, which lower the ignition probability. This phenomenon is partially at the origin of the large percentage of misfires observed for this condition.

6 LIQUID PHASE VISUALISATION

The liquid phase of the fuel jet was visualised by collecting light scattered by the droplets in the chamber. We used a laser sheet in the green region (532 nm) from a YAG laser that crosses the chamber vertically through the transparent piston. We collected the light orthogonally through the side window placed in the cylinder head. In Figure 12, we show images averaged over 100 cycles in the three selected conditions, at crank angles from 11 to 7° BTDC, that is just after spark timing.

A strong liquid concentration is effectively observed in condition B where the delay between injection and ignition is small. In the two others cases with earlier injection, liquid is much less concentrated and never located at the electrode gap. The granular zone on condition C corresponds to large and slow droplets that are introduced after the main because of an injector needle rebound.

7 FUEL FIELD DESCRIPTION

The engine is fired every fourth cycle to reject the influence of recycled burnt gas, and 300 cycles are recorded. The engine is running without combustion and laser-induced fluorescence is applied on iso-octane seeded with the exciplex mixture to quantify the fuel/air ratio field in a vertical plane.

7.1 Fuel / Air Ratio Quantification Method

Quantification requires correction for laser power, laser intensity profile, local engine conditions (temperature and pressure) and camera sensitivity. Our procedure is based on

TABLE 4

Main combustion results in the three selected operating conditions

	Injection timing (°BTDC)	Spark timing (°BTDC)	Misfires (%)	BMEP (MPa)	rms(BMEP)/BMEP, excluding misfires (%)	Comments
Condition A	25	11	0	.298	5.7	Optimal, maximum BMEP, stable combustion, no misfire
Condition B	21	11	58	.290	8.9	Many misfires
Condition C	31	11	0	.238	21	Slow and unstable combustion, lower BMEP, no misfire

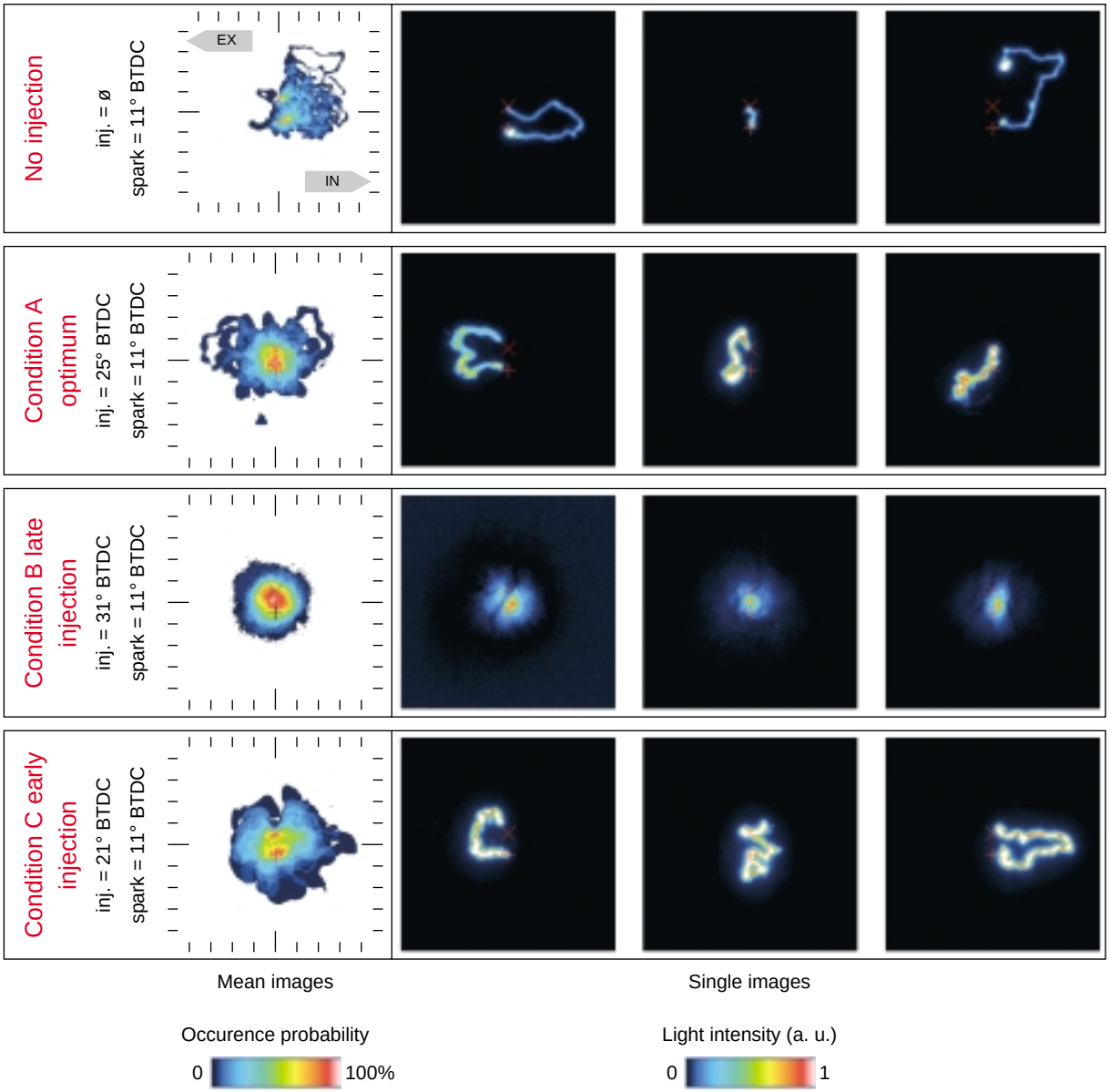

Figure 11

Visualisation of the ignition spark.

that developed by Lozano *et al.* [16]. Therefore, each test is quantified using another reference test with assumed homogeneous concentration in the chamber, keeping constant all the other parameters. The reference test is taken for each image angle, by injecting during the intake stroke, at 300° BTDC. All the parameters dealing with the optical technique, such as intensifier gain, lens aperture, laser power, were kept rigorously constant between reference and signal images, so that the quantification is more reliable.

In a first step we verified that the fluorescence signal is proportional to the fuel/air ratio by injecting fuel quantities corresponding to fuel/air ratios ranging from 0.5 to 2. One can see that the signal is a linear function of the fuel/air ratio up to 1.5 (*Fig. 13*). Laser absorption can explain the deviation from the linear curve above this limit. We can conclude that for our study the linear trend is a good approximation.

In a second step, the correction for local laser intensity, vignetting and collection efficiency was tested. As shown by Figure 14, dividing a raw signal image by a reference image can correct for all these effects, since a very homogeneous intensity is seen on the resulting image.

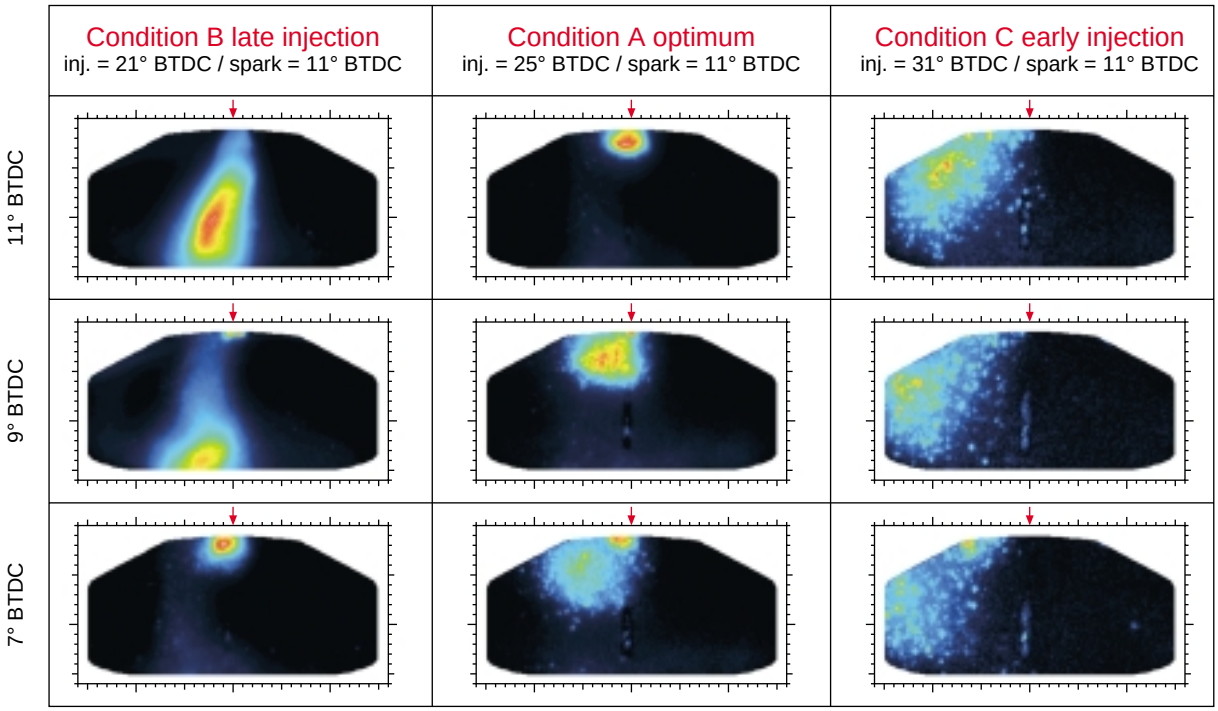

Figure 12

Average images of the liquid fuel in the chamber (obtained by light scattering).

The corrected and quantified images shown hereafter will use the same colour palette, with green corresponding to the stoichiometric conditions. Iso-contours are drawn at 0.8, 1.1 and 1.5 in order to locate the lean, optimal and rich conditions, as shown in Figure 15. The locations of the electrode gap and the injector nozzle are also indicated.

The method used to calculate the fuel/air ratio from the fluorescence signal has some limitations. It should be noted that the quantification procedure assumes that the fluorescence yield is identical in the reference and the signal images. However, local temperature in evaporating spray is lower, and can influence the local fluorescence. Another factor, droplet concentration can be very high in the spray, for small delays after injection onset. Thus, the laser sheet reaches fuel that is mainly liquid and can be scattered. Since the calibration curve is done with a reference test with only vapour fuel, the F/A ratio calculated can be affected by a large error. To conclude, the quantification is rather reliable at long times after injection onset, where low droplet concentration and sufficient vapour spreading are observed.

7.2 Fuel / Air Ratio Map Results

We show the mean fuel/air ratio maps, as calculated from laser-induced fluorescence images and the histograms of the cycle-to-cycle fuel/air ratio near the spark location in Figures 16 to 18. The fuel/air ratio at spark location was calculated for each single image, by averaging the pixel intensity in a 4 mm diameter disk centred on the electrode gap. We will focus the discussion on the F/A ratio at 2 degrees after spark timing (9° BTDC), because it lies right in the spark duration.

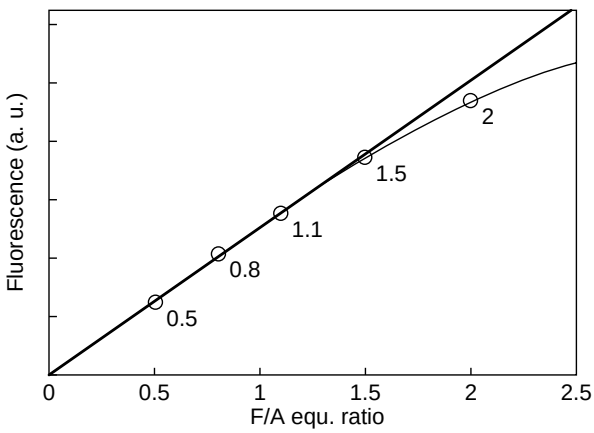

Figure 13

Influence of the fuel/air equ. ratio on the fluorescence signal in the case of homogeneous mixtures.

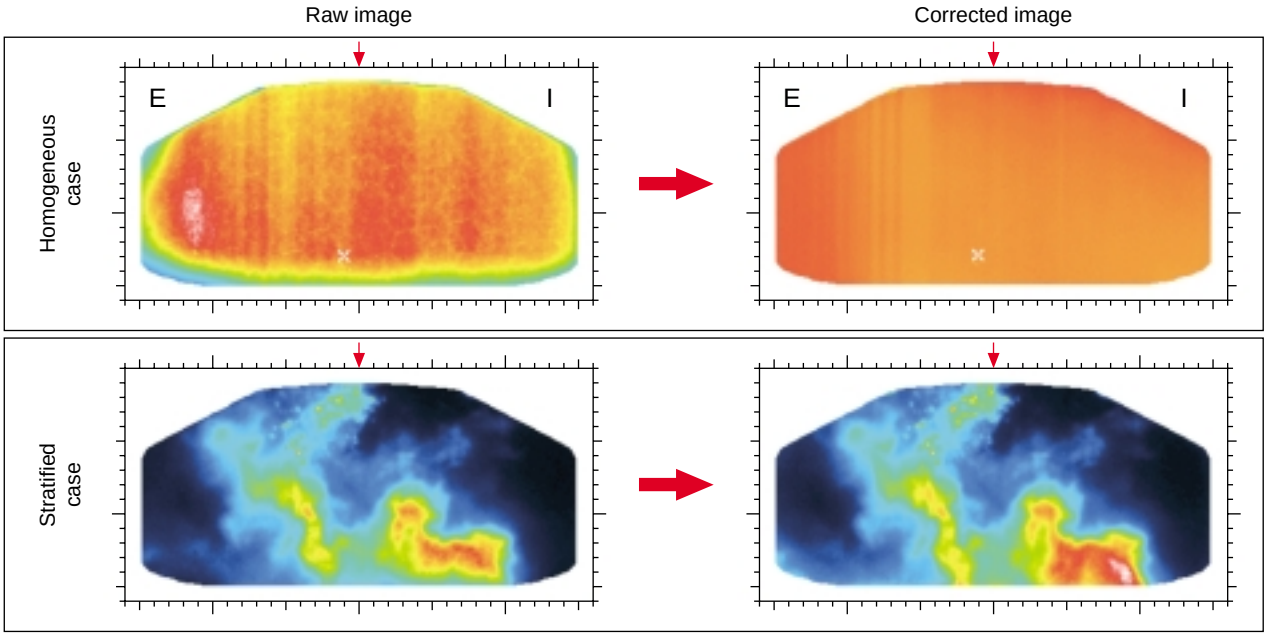

Figure 14

Demonstration of the image processing.

The general feature is that the spray impinges the piston surface in a short delay, and that the fuel jet forms a toroidal cloud that develops horizontally along this surface. After the impact, the rich pocket lying near the piston surface is convected by the tumbling flow, towards the intake valve side.

In the optimum condition A, ignition takes place well after the end of injection, in the tail of the jet. The rich zone moves rather slowly from the piston surface, so that favourable conditions are obtained at the spark location and timing: nearly stoichiometric conditions, and a weak spatial gradient. Furthermore, the fuel/air ratio histogram is not very wide, spanning from 0.5 to 2 at 9° BTDC.

The condition B with late injection is obviously too rich. The spray has not diffused very much in the chamber, and fuel stratification is strong. Ignition occurs during the main injection phase, so that the fuel/air ratio exceeds 2 in a majority of cycles. Images of the liquid phase already showed high liquid concentration in the electrode gap zone. This could explain why the fuel/air ratio is very high. It even exceeds the upper limit of the fluorescence calibration curve, resulting in saturation inside the images. This correlates with the high percentage of misfiring cycles in this condition.

The condition C with early injection offers too poor condition for combustion. The impact between the spray and the piston surface is well achieved at the time of ignition. The mean fuel/air ratio is equal to 0.7 and cycle-to-cycle variations between 0.3 and 1.2 are observed at 2 degrees after spark timing. This results from a long delay between injection and ignition, which allows the fuel to spread out in a large part of the chamber. Very lean conditions in the electrode gap vicinity lead to slow combustion in a large percentage of cycles.

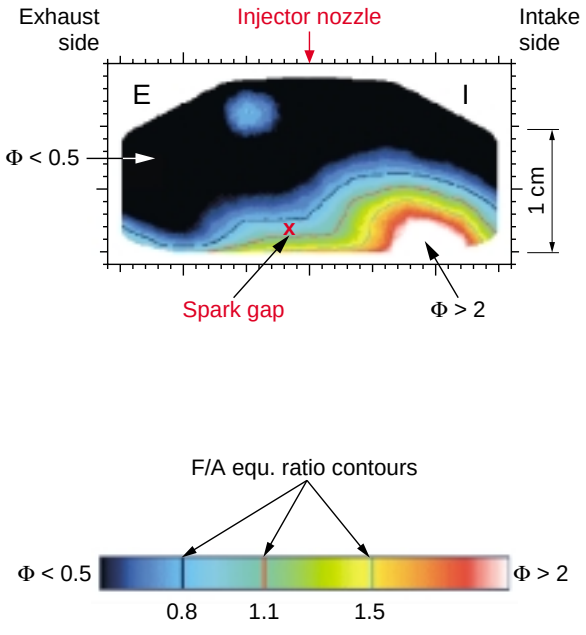

Figure 15

Explanation of fuel/air equ. ratio maps plotted.

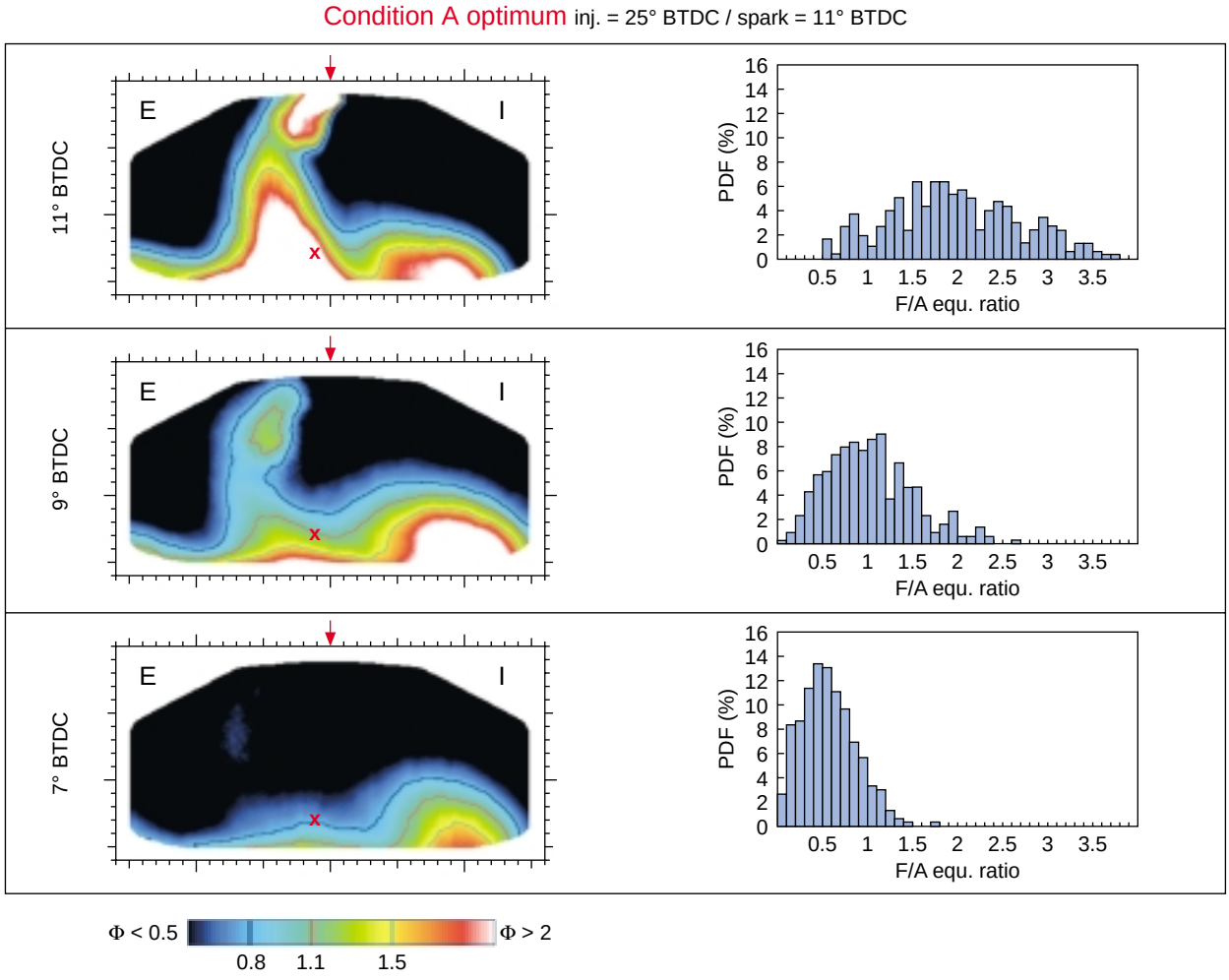

Figure 16

Mean fuel/air equ. ratio map and histogram in the ignition zone in optimal condition A.

Besides the fuel/air ratio histograms, we determined the probability that the mixture will be lean, stoichiometric or rich in the electrode gap vicinity (*Fig. 19*). In condition A, it appears that the maximum probability to have a stoichiometric mixture is in the optimum case, just in the ignition window, around 9 or 10° BTDC. In condition B, the vast majority of cycles are very rich, at spark timing (11° BTDC). Ignition should be retarded up to 7° BTDC approximately to find stoechiometric mixture. This confirms that the delay between injection and ignition must be about 13 CAD to get a stable combustion. In condition C, the majority of cycles are lean at the time of ignition. In a first phase, the percentage of cycles with stoichiometric mixture diminishes with time, because fuel moves towards the piston surface. In a second phase, it increases again, because the impact of the fuel jet on the piston surface generates a vortex of fuel vapour that gradually thickens, and reaches the electrode gap.

7.3 Correlation Between Stratification and Combustion

It is interesting to correlate the fuel/ratio near the ignition point with combustion, as performed in the work of Wagner *et al.* [17]. First we qualitatively correlate the fuel distribution with the heat release curves. The pressure cycles acquired for the BMEP measurements were analysed with a two-zone thermodynamic model, which provides the burnt fraction *versus* crank-angle. We examine in this chapter the qualitative correlation between the histograms of 5% and 50% burnt fraction crank angles—called CA5 and CA50—with the fuel stratification observed at ignition

The histogram of CA5 displayed in Figure 20 shows that the initiation duration is very short (11 CAD) and stable in the optimum case A. This confirms the good conditions achieved with a fuel/air ratio around 1 and relatively low

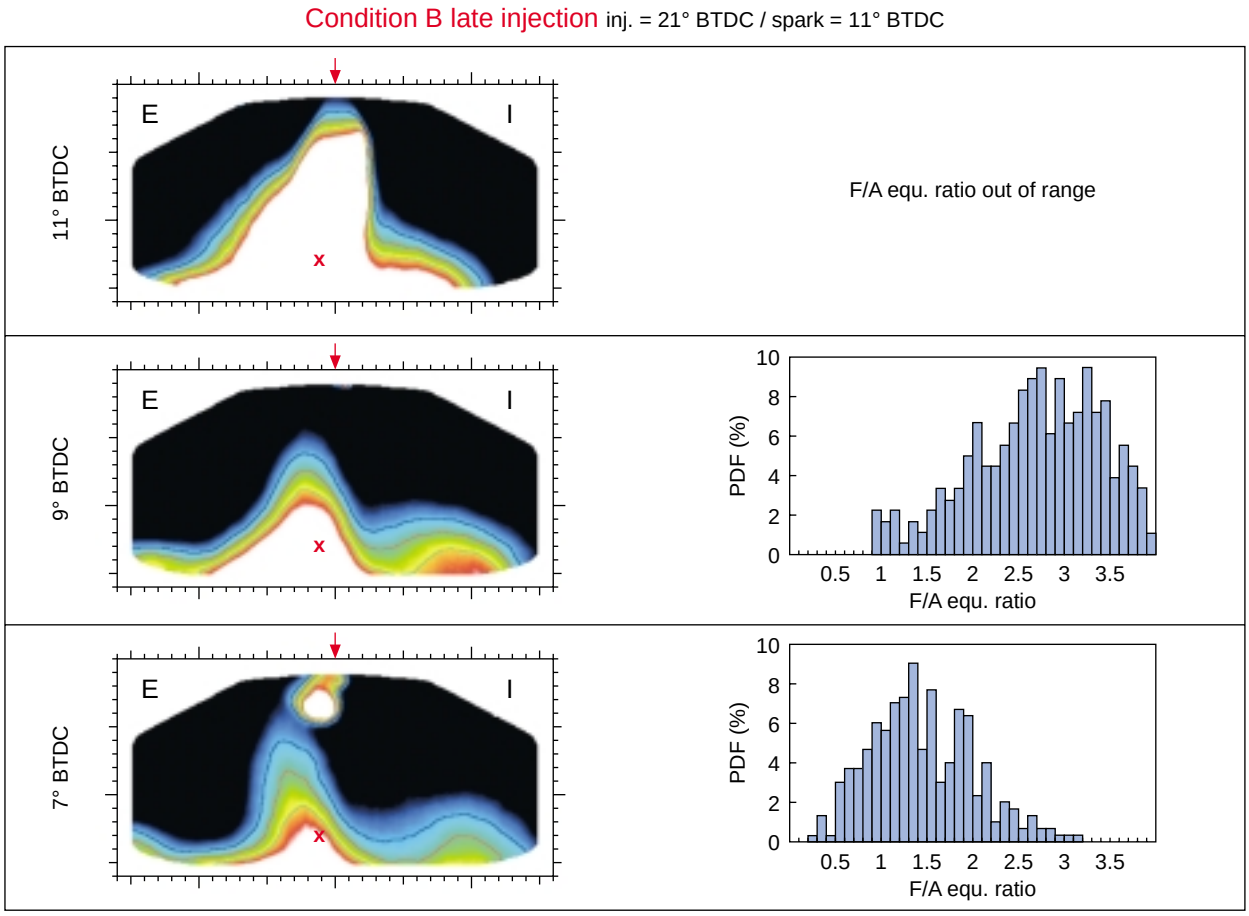

Figure 17

Mean fuel/air equ. ratio map and histogram in the ignition zone in condition B (late injection).

cycle-to-cycle fluctuations. The heat release is correctly phased in the engine cycle, since average CA50 is 367 CAD, and is also very stable.

In condition B, initiation is less stable (misfires are not plotted in the graph). This is correlated with high liquid concentration in the electrode gap. Here we see that when ignition succeeds, combustion is even slower than in the optimum condition, CA50 is equal to 372 CAD. This means that fuel mixing with ambient air is too weak.

In condition C, CA5 fluctuations are higher than in the optimum case. CA5 can reach 365 CAD in some cycles, as a consequence of very lean conditions at the spark. Moreover the propagation phase is very unstable, as CA50 can exceed 400 CAD. The key parameter is the fuel/air ratio in the fuel jet. In some cycles, the mixture is too lean to insure correct flame propagation. Thus, fuel spreading in the chamber is very probably too high. Other work demonstrate that zones with F/A ratio lower than 0.3 can hardly been burned [18]. These represent a large percentage of the fuel injected in this condition C, and can contribute to slow flame propagation and even local flame extinction.

Therefore, we can conclude that combustion history is very dependent on the fuel/air ratio field generated by the injection process and the impact of the fuel jet on the piston wall in our configuration. The optimum condition corresponds to the case with a mean fuel/air ratio closest to 1, the least cyclic variability, and a medium stratification in the chamber.

7.4 Cycle-to-Cycle Correlation between Fuel Concentration and Combustion

In a few tests, simultaneous imaging of fuel concentration field just before combustion and pressure recording during combustion were done. We recall that 3-pentanone was the tracer used, because the engine was fed with air in order to burn the fuel. Cyclic correlation between fuel field in the window and combustion were possible in all the three conditions. However, in condition B the concentrations were too high to provide a clear correlation between fuel concentration and combustion. Local parameters, such as electrode wetting were not caught by the planar laser-induced fluorescence method. The most demonstrative case was

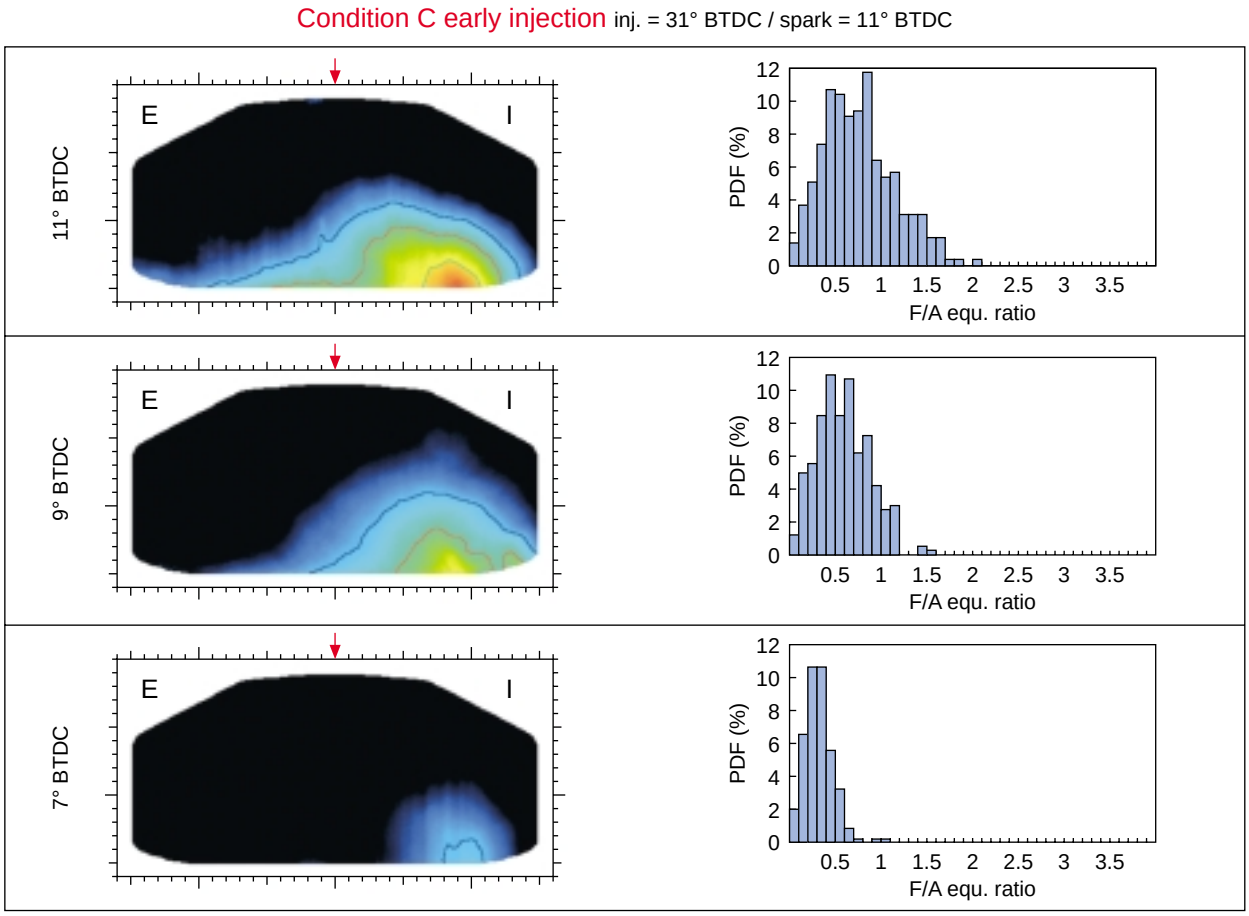

Figure 18

Mean fuel/air equ. ratio map and histogram in the ignition zone in condition C (early injection).

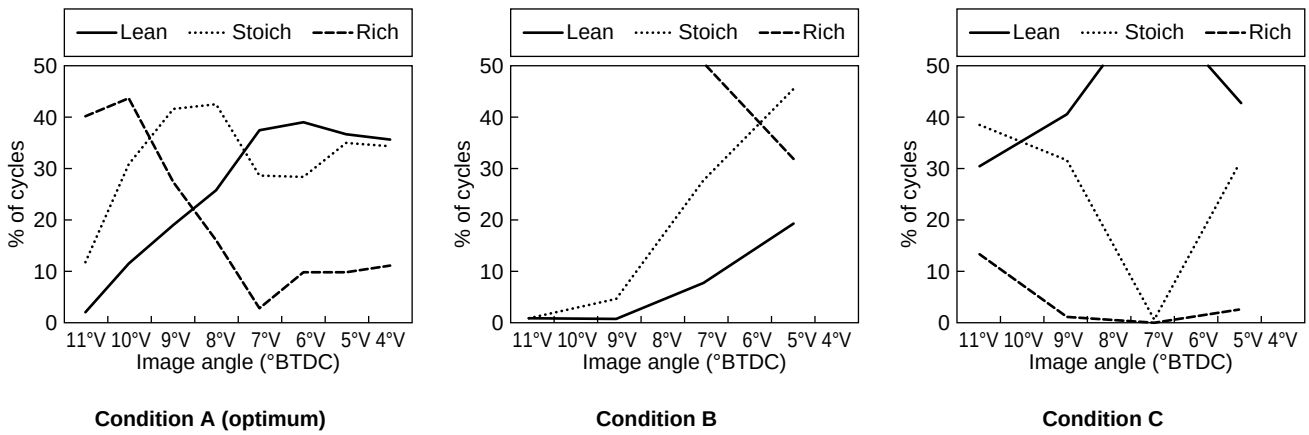

Figure 19

Percentage of cycles with lean, stoichiometric or rich conditions in the electrode gap *versus* crank angle.

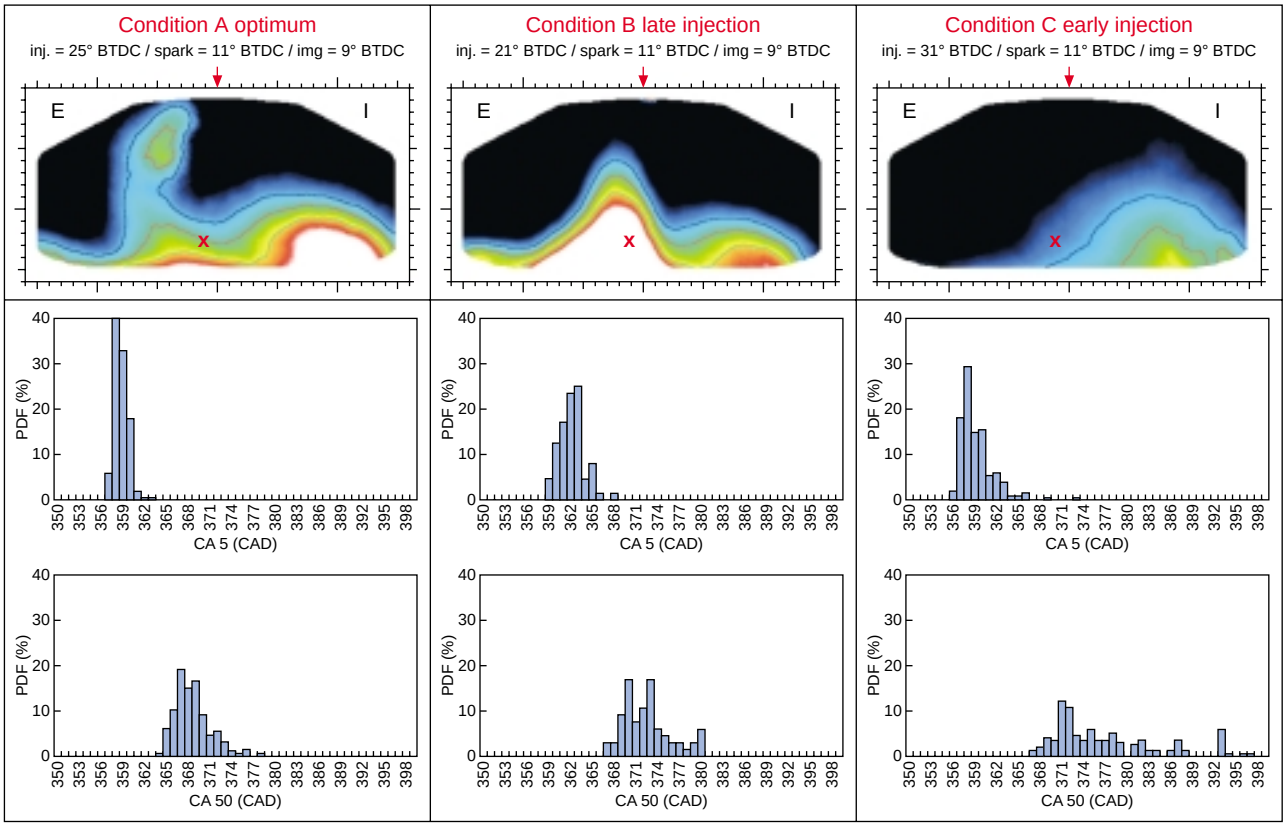

Figure 20

Correlation between fuel/air equ. ratio map at 9° BTDC and combustion (initiation 5% burnt, propagation 50%).

found in condition C, which will be examined hereafter. In a collection of cycles we selected several cycles with CA5 higher than 367 CAD, *i.e.* with a long initiation of combustion (shown in green in the CA5 histogram in Figure 21) and took the corresponding fuel field measured by laser induced fluorescence. Images from cycles with normal initiation (CA5 equal to 359 CAD) are plotted against them, on the left side. The fuel/air ratio is obviously much lower in all the cycles with large CA5. This directly demonstrates that the fuel/air ratio at the ignition point is a key parameter for initiating correctly the engine charge in stratified charge direct injection gasoline engines.

CONCLUSION

Among the tracers tested, the best ones for doing laser-induced fluorescence in an optical engine are the exciplex triethylamine/benzene mixture without oxygen for tests without combustion, and 3-pentanone for tests with combustion. The delay between injection and ignition is the most important parameter that controls the combustion of a stratified charge gasoline engine. Optimal combustion corresponds to near stoichiometric conditions at the spark location, and also to the maximal probability of having stoichiometric conditions in the same place. A small delay between injection and combustion leads to wetting of the spark plug electrodes by liquid fuel, to the absence of spark in some cycles, and to a lot of misfires. Conversely, a long delay yields to a lean mixture at the spark location, and an excessively dilute mixture in the whole chamber. This leads to very unstable combustion, cycles with slow combustion, and also to some incomplete combustion.

ACKNOWLEDGEMENTS

This work was supported by the *Groupement Scientifique Moteurs* (including *Peugeot SA* , *Renault* and *IFP*), *Siemens Automotive* and the *French ministère de l'Industrie*. Fruitful discussions with P. Gastaldi from *Renault* and T. Duverger from *PSA* are acknowledged.

REFERENCES

1 Akihiko, K., Urushihara, T., Itoh, T. and Takagi, Y. (1999) Characteristics of Mixture Formation in a Direct-Injection SI Engine with Optimized in-Cylinder Swirl Air Motion. *SAE Paper 1999-01-050.*

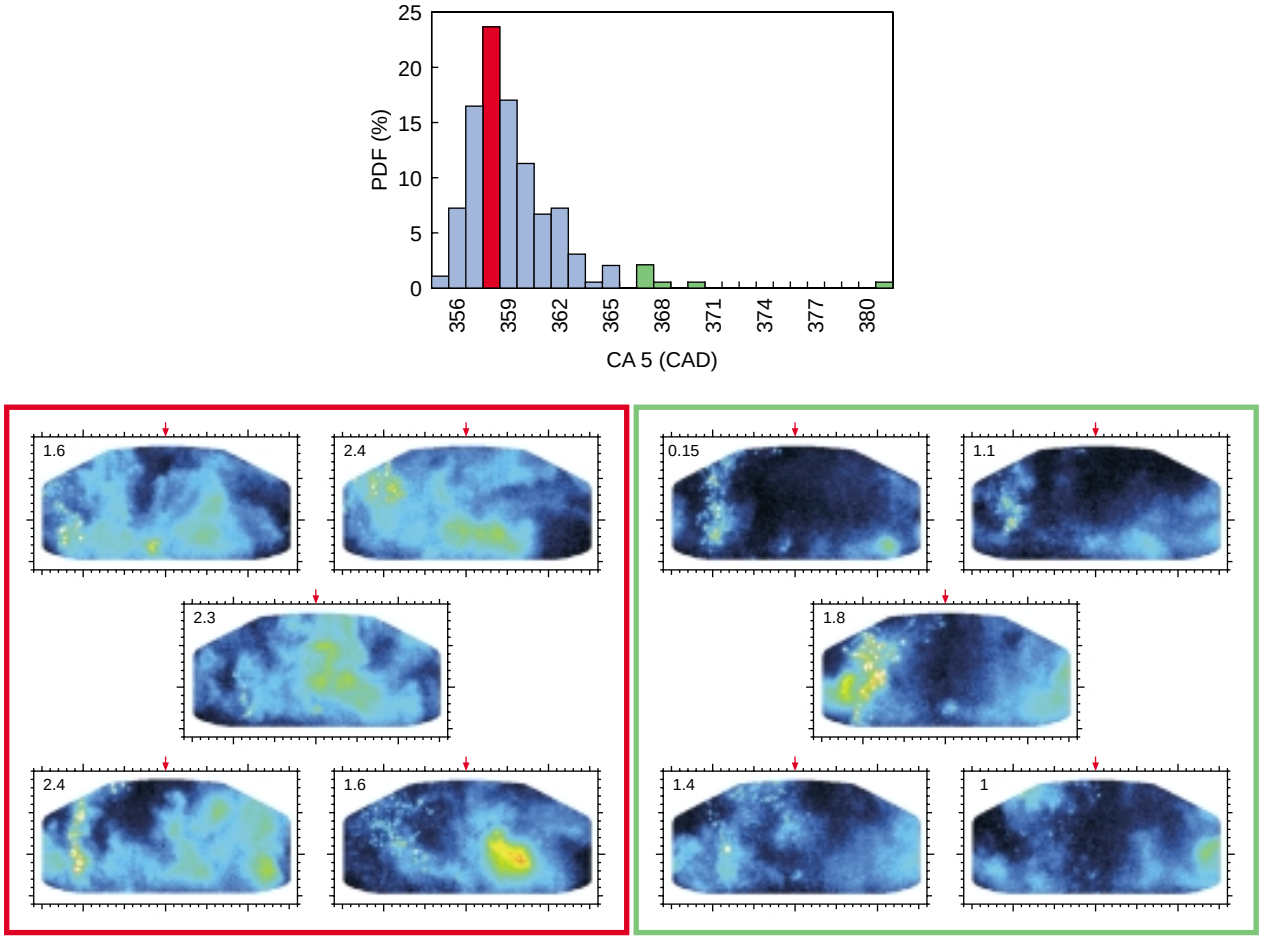

Figure 21

Histogram of CA5 and fuel/air equ. ratio maps in some cycles with quick combustion (left: CA5 = 358) or slow combustion (right: CA5 > 365), in condition C.

2 Fraidl, G. K., Piock, W. F. and Wirth, M. (1996) Gasoline Direct Injection: Actual Trends and Future Strategies for Injection and Combustion Systems. *SAE Paper 960465.*

3 Harada, J., Tomita, T., Mizuno, H., Mashiki, Z. and Ito, Y. (1997) Development of Direct-Injection Gasoline Engine. *SAE Paper 970540.*

4 Kume, T., Iwamoto, Y., Iida, K., Murakami, M., Akishino, K. and Ando, H. (1996) Combustion Control Technologies for Direct Injection SI Engine. *SAE Paper 960600.*

5 Iwamoto, Y., Noma, K., Nakayama, O., Yamauchi, T. and Ando, H. (1997) Development of Gasoline Direct Injection Engines. *SAE Paper 970541.*

6 Takagi, Y., Itoh, T., Muranaka, S.,Iiyama, A., Iwakiri, Y., Urushihara, T. and Naitoh, K. (1998) Simultaneous Attainment of Low Fuel Consumption, High Output Power and Low Exhaust Emissions in Direct-Injection SI Engines. *SAE Paper 980149.*

7 Castagne, M., Cheve, E., Dumas, J.P. and Henriot, S. (2000) Advanced Tools for Analysis of Gasoline Direct Injection Engines. *SAE Paper 2000-01-1903.*

8 Gold, M., Li, G., Sapsford, S. and Stokes, J. (2000) Application of Optical Techniques to the Study of Mixture Preparation in Direct Injection Gasoline Engines and Validation of a CFD Model. *SAE Paper 2000-01-0538.*

9 Münch, K.U., Kramer, H. and Leipertz, A. (1996) Investigation of Fuel Evaporation Inside the Intake of a SI Engine Using LIEF with a New Seed. *SAE Paper 961930.*

10 Fröba, A.P., Rabenstein, F., Münch, K.U. and Leipertz, A. (1998) Mixture of TEA and Benzene as a New Seeding Material for the Quantitative Two-Dimensional LIEF Imaging of Vapor and Liquid Fuel Inside SI Engines. *Comb. & Flame,* **112**,199-209.

11 Deschamps, B., Lessart, P. and Ricordeau, V. (1998) Diagnostics optiques de l'injection directe d'essence. *IFP Report 44755.*

12 Deschamps, B., Ricordeau, V., Depussay, E. and Mounaïm-Rousselle, C. (1999) Combined Catalytic Hot Wires Probe and Fuel-Air-Ratio-Laser Induced-Exciplex Fluorescence Air/Fuel Ratio Measurements at the Spark Location Prior to Ignition in a Stratified GDI Engine. *SAE Paper 1999-01-3536.*

13 Lawrenz, W., Kohler, J., Meier, F., Stolz, W., Wirth, R., Bloss, W.H., Maly, R.R., Wagner, E. and Zahn, M. (1992) Quantitative 2D LIF Measurements of Air/fuel Ratios During the Intake Stroke in a Transparent SI Engine. *SAE Paper 922320*.

14 Lefebvre, A.H. (1989) *Atomisation and Sprays*, Hemisphere Publishing.

15 Le Coz, J.F. (1998) Comparison of Different Drop Sizing Techniques on Direct Injection Gasoline Sprays. *9th Int. Symp. on Applications of Laser Techniques to Fluid Mechanics*, Lisbon, Portugal.

16 Lozano, A., Yip, B. and Hanson, R.K. (1992) Acetone: a Tracer for Concentration Measurements in Gaseous Flows by Planar Laser-Induced Fluorescence. *Exp. in Fluids*, **13**, 369-376.

17 Wagner, V., Ipp, W., Wensing, M. and Leipertz, A. (1999) Fuel Distribution and Mixture Formation Inside a Direct-Injection SI Engine Investigated by 2D Mie and LIEF Techniques. *SAE Paper 1999-01-365*.

18 Strand, T.E., Rothamer, D.A. and Ghandhi, J.B. (2001) Flame Structure Visualization of Stratified Combustion in a DISI Engine Via PLIF. *SAE Paper 2001-01-3649*.

Final manuscript received in October 2002